Supplementary Material

Borax crosslinked hydrogel of 2-methyl-2-propene-1-sulphonate grafted onto guar gum for removing cationic dyes and Cr^{6+} ions

Kavita Chauhan, Ghanshyam S. Chauhan, Sandeep Chauhan*

Department of Chemistry, Himachal Pradesh University, Summerhill, Shimla, Himachal -Pradesh, India-171005.
*Correspondence: sandeepchauhanin2020@gmail.com (Sandeep Chauhan)

S1 Swelling percentage determination

At room temperature, 0.5 g of the GG@MPS@H was immersed in 50 mL of DW in a 100 mL beaker. The swollen hydrogel was periodically removed, cleaned with filter paper, and weighed. The percent swelling (P_s) was computed using Eq. S1

$$\text{Percent swelling } (P_s) = \frac{w_2 - w_1}{w_1} \times 100 \quad \textbf{(S1)}$$

Where, w_1 and w_2 denote the weight of the dried and swelled hydrogel, respectively.

S2. Adsorption kinetics, thermodynamics and adsorption isotherms

Various non-linear kinetic models, including pseudo-first-order (PFO) [58], pseudo-second-order (PSO) [59], and Elovich [60], were applied to determine the adsorption mechanism [Table S1]. Similarly, the thermodynamic parameters, including standard Gibb's free energy change (ΔG°), standard enthalpy change (ΔH°), and standard entropy change (ΔS°) were calculated. The ΔG° was calculated by using the following equation:

$$\Delta G^\circ = -RT\ln K_c \quad \textbf{(S2)}$$

Where R is the universal gas constant (8.314 $JK^{-1}mol^{-1}$), T is the absolute temperature (K), and K_c is the equilibrium constant. The other two thermodynamic parameters, ΔH° and ΔS° were calculated by using the equation:

$$\ln K_c = \Delta S^\circ/R - \Delta H^\circ/RT \quad \textbf{(S3)}$$

To determine the value of ΔH° and ΔS° from the slope and intercept, a graph was plotted between InKc and 1/T**.** The mechanism of the adsorption of adsorbate onto the adsorbent was

analyzed by using the non-linear Langmuir [63], Freundlich [62], and Temkin isotherm models [61](Table S2).

S3. Adsorption kinetics and isotherms evaluation by non-linear models

Error functions are used to check the fitting of the experimental data of adsorption kinetics and isotherm model with the theoretical data. For this purpose, the error functions i.e. Chi-square (χ^2) [64], root mean square error (RMSE) [66], and normalized standard deviation Δq% were used [65]. The following formulas were used:

$$\chi^2 = \sum \frac{[q(exp) - q(cal)]^2}{q(\text{exp})} \qquad (\mathbf{S4})$$

$$\Delta q\% = 100 \times \sqrt{\frac{\sum(\frac{q(exp) - q(cal)}{q(\text{exp})})^2}{N-1}} \qquad (\mathbf{S5})$$

$$\text{RMSE} = \sqrt{\frac{1}{N-1}} \sum [q(exp) - q(cal)]^2 \qquad (\mathbf{S6})$$

Herein, *q (exp)* = experimental adsorption capacity, *q (cal)* = ealculated adsorption capacity, N = number of data points.

The small values of χ^2, RMSE and Δq% more proximity between experimental and calculated data of kinetics and isotherm models. All non-linear models were compared by analysing the data of the coefficient of determination (R^2), Δq%, χ^2, and RMSE.

Table S1

Design of experiment for the synthesis of GG@MPS@H and corresponding P_r values

Run	GG (g)	MPS (g)	Borax (g)	P_r of CV dye	P_r of MB dye	P_r of Cr^{6+} ions
1.	1.000	1.000	0.100	93.65	92.92	91.84
2.	1.000	2.000	0.150	92.67	92.41	90.23
3.	1.000	0.500	0.075	91.23	92.43	91.23
4.	1.000	1.500	0.125	92.34	91.45	89.43
5.	***1.000***	***1.500***	***0.125***	***94.48***	***93.74***	***92.82***
6.	1.000	1.500	0.125	91.32	90.52	89.12
7.	1.000	1.500	0.125	90.12	89.46	88.34
8.	1.000	1.500	0.075	91.43	92.14	90.12
9.	1.000	1.500	0.200	89.45	89.21	86.32

S4 Swelling behaviour of the GG@MPS@H

An essential feature of hydrogel for its use is its capacity to swell. Dynamic equilibrium governs the hydrogel's swelling behaviour. Water molecules can slowly permeate into the network of GG@MPS@H when submerged in distilled water, increasing the hydrogel's volume. The hydrogel's rate of swelling increased rapidly during the first phase, reaching equilibrium state at 24 h. The swelling percentage of the hydrogel rises in proportion to the density of hydrophilic groups in the hydrogel that includes the high number of ionisable sulphate groups and hydroxyl group present in GG@MPS@H (Fig. S1b).

Table S2

Kinetic models and their equation in non-linear form

Non-linear kinetic models	Equations	Parameters
Pseudo-first order	$q_t = q_e\ (1\text{-}e^{-k1t})$	q_t (mg/g) = adsorption capacity at the time 't' q_e (mg/g) = equilibrium adsorption capacity k_1 (min^{-1}) = Pseudo-first order rate constant
Pseudo-second order	$q_t = \frac{k_2 q_e{}^2 t}{1 + k_2 q_e t}$	q_t (mg/g) = adsorption capacity at the time 't' q_e (mg/g) = equilibrium adsorption capacity k_2 (g/mg min) = Pseudo-second order rate constant
Elovich	$q_t = \frac{1}{\beta} \ln(1+\alpha\beta t)$	q_t (mg/g) = adsorption capacity at the time 't' α (mg/g min) = Elovich initial adsorption rate β (g/mg) = desorption constant

Table S3

Isotherms models and their equation in non-linear form

Non-linear isotherms	Equations	Parameters
Langmuir isotherm model	$q_t = \frac{q_m B C_e}{1 + B C_e}$	q_t(mg/g) = adsorption capacity at the time 't' C_e (mg/g) = equilibrium adsorption capacity q_m (mg/g) = Maximum adsorption capacity B = Langmuir constant
Freundlich isotherm model	$q_t = K_F C_e^{1/n}$	q_t (mg/g) = adsorption capacity at the time 't' C_e (mg/g) = equilibrium adsorption capacity K_F = Freundlich constant related to adsorption capacity 1/n = Freundlich constant related to adsorption intensity
Temkin isotherm	$q_t = \beta \ln(k_T C_e)$ Where, $\beta = \frac{RT}{b}$	q_t (mg/g) = adsorption capacity at the time 't' C_e (mg/g) = equilibrium adsorption capacity b = Temkin constant K_T = equilibrium binding constant T = the temperature R = universal gas constant

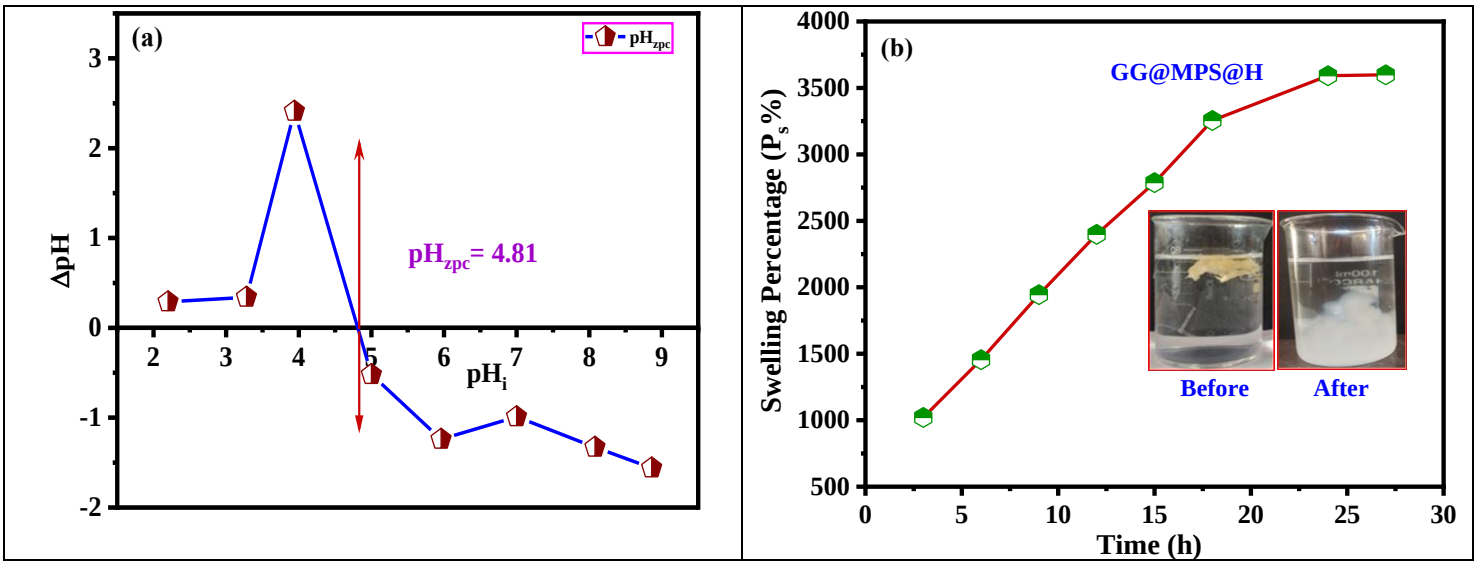

Fig. S1. (a) pH_{zpc} of GG@MPS@H, (b) swelling percentage graph of GG@MPS@H (c) UV-vis spectrum of individual MG dye removal

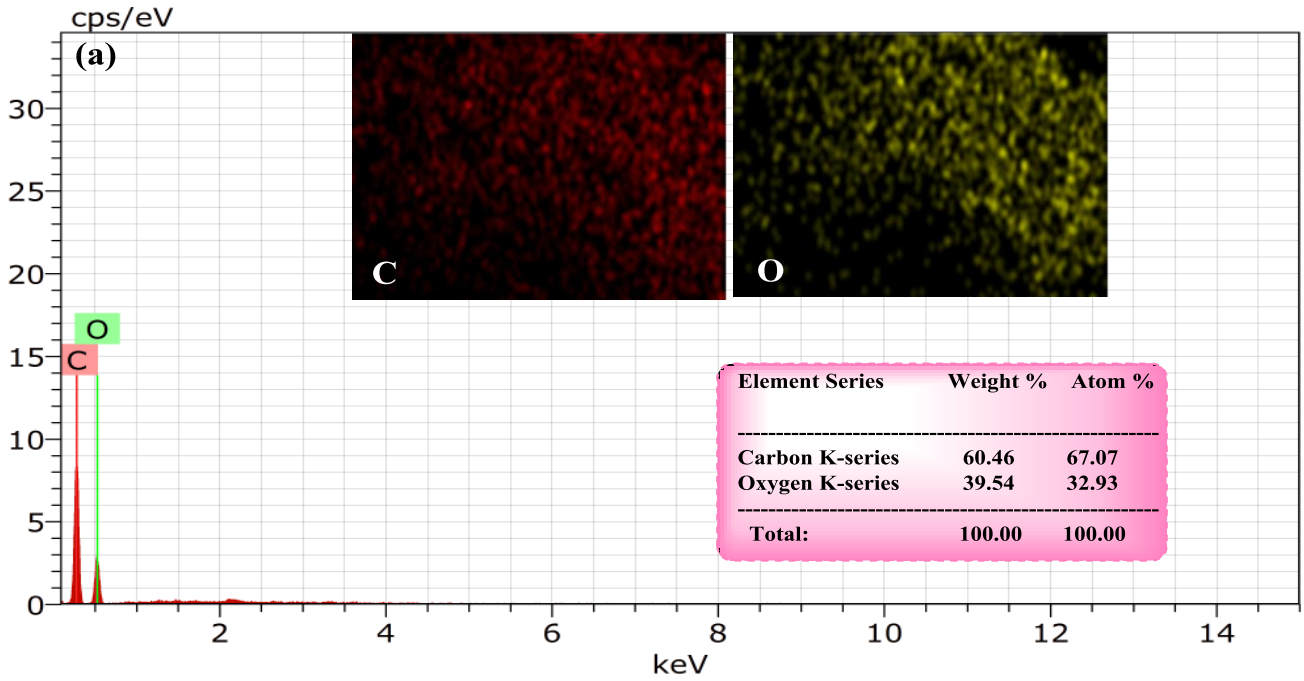

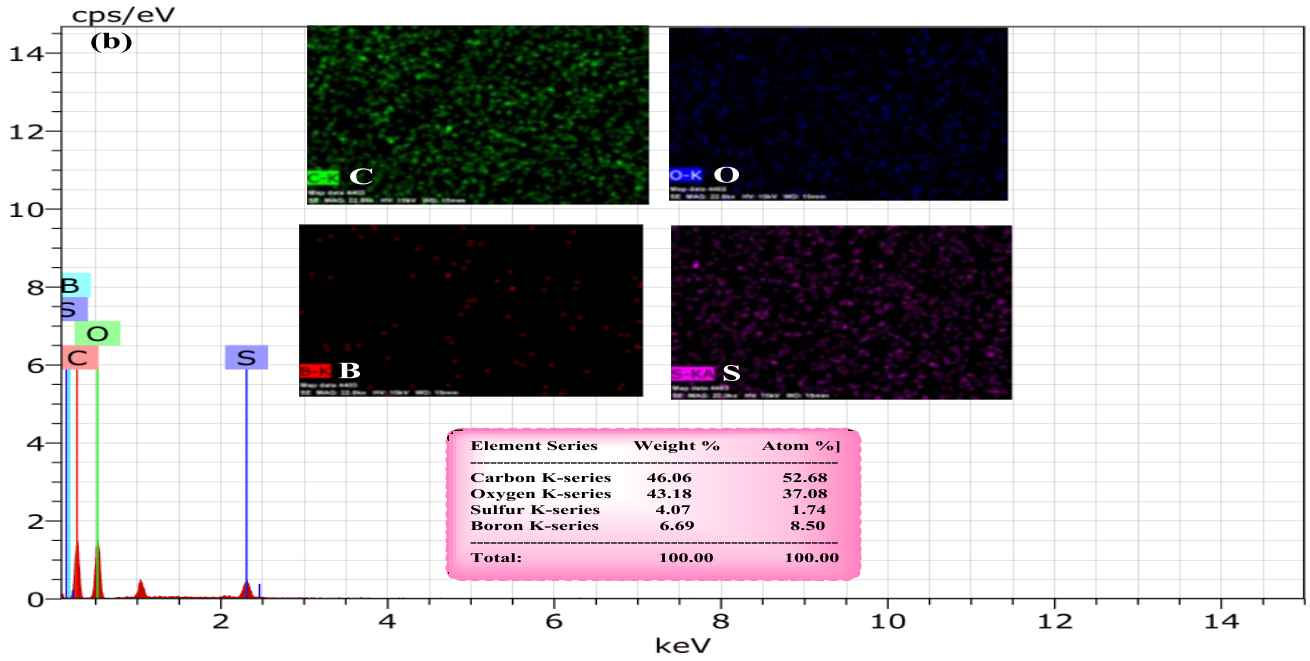
cps/eV
(b)
C
O
B
S
C
O
S
keV
Element Series Weight % Atom %
Carbon K-series 46.06 52.68
Oxygen K-series 43.18 37.08
Sulfur K-series 4.07 1.74
Boron K-series 6.69 8.50
Total: 100.00 100.00

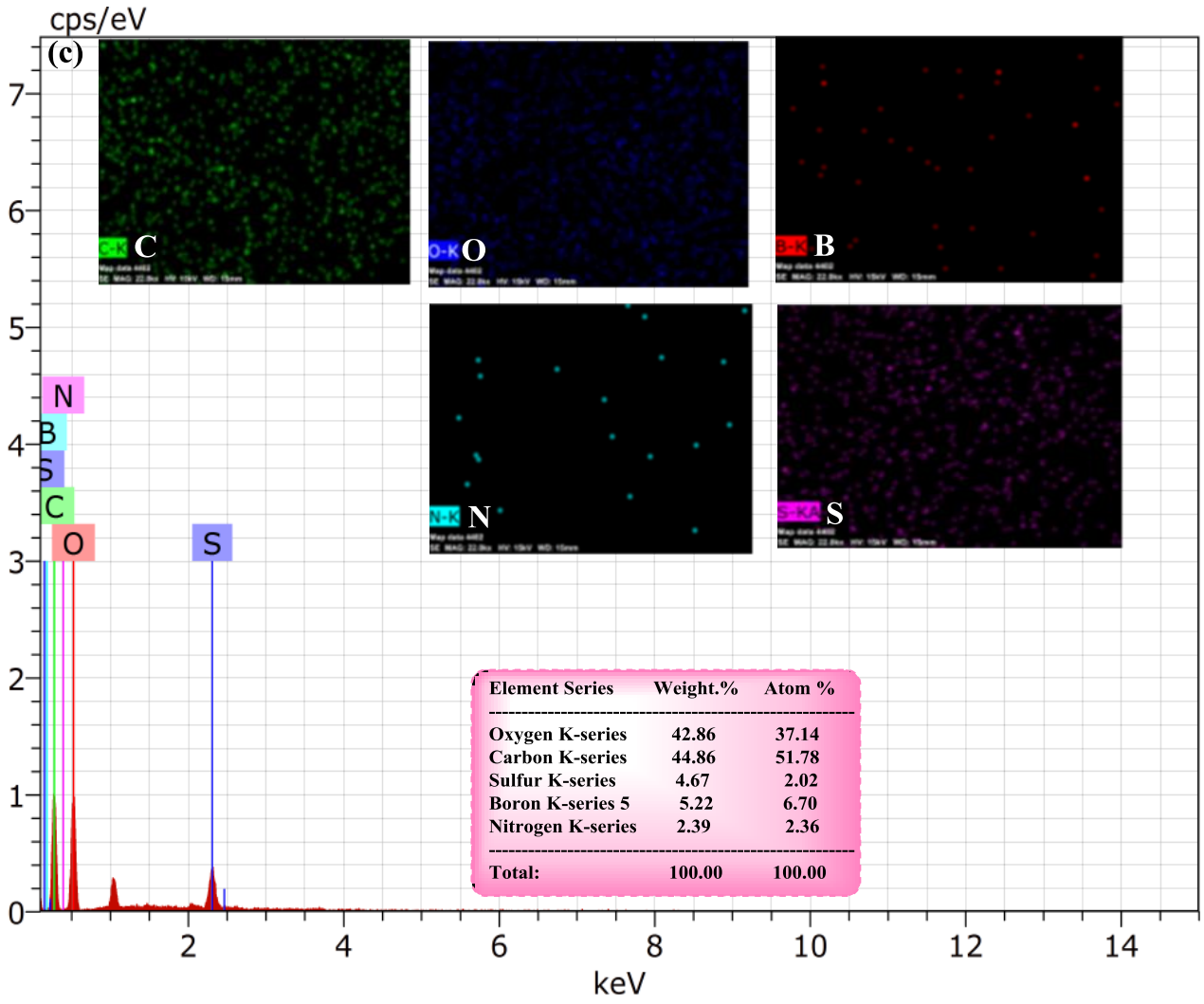
cps/eV
(c)
C
O
B
N
S
N
B
S
C
O
S
keV
Element Series Weight.% Atom %
Oxygen K-series 42.86 37.14
Carbon K-series 44.86 51.78
Sulfur K-series 4.67 2.02
Boron K-series 5 5.22 6.70
Nitrogen K-series 2.39 2.36
Total: 100.00 100.00

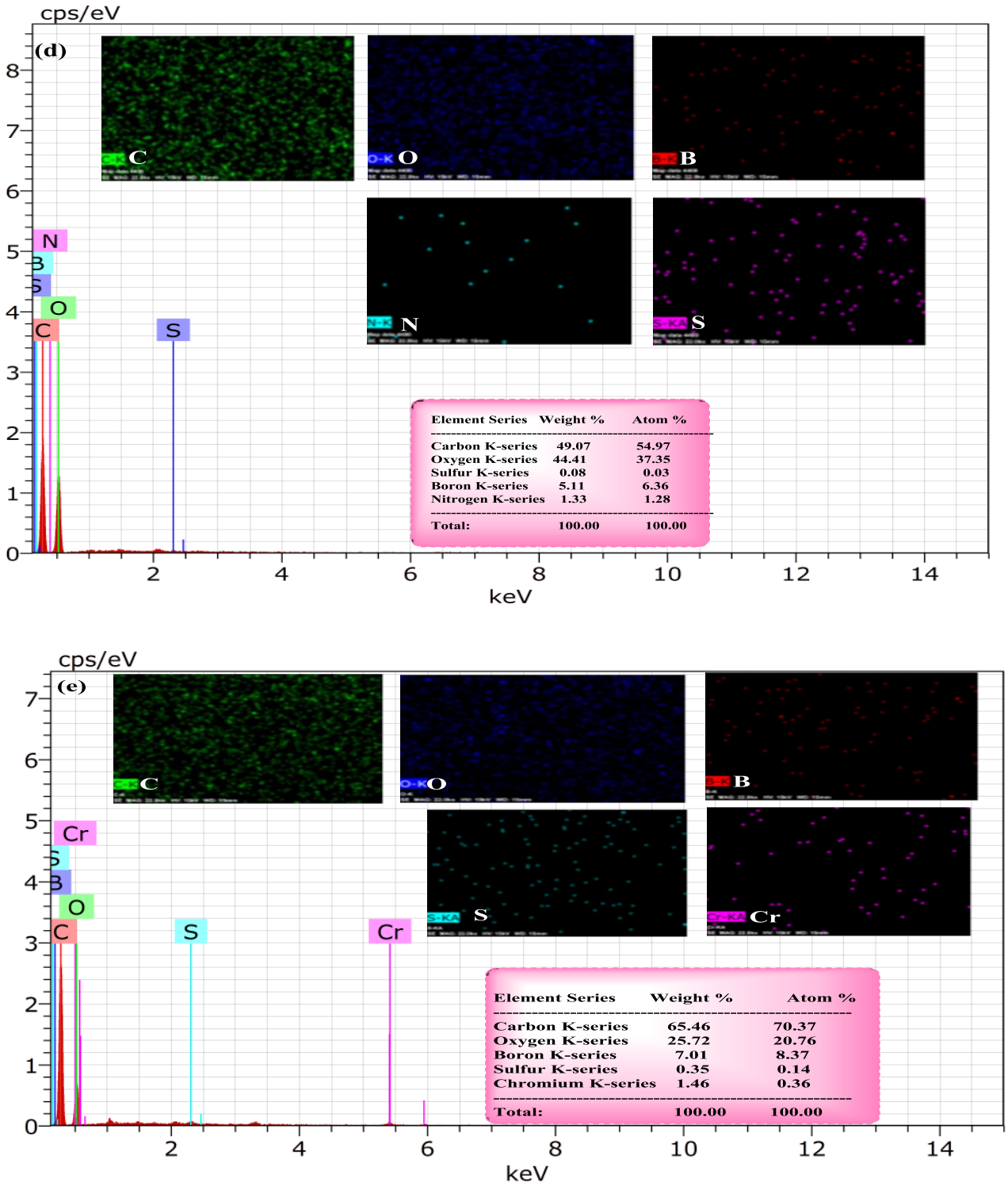

Fig. S2. EDX profiles and weight %ages of elements on the surface of (a) GG, (b) GG@MPS@H, (c) CV-loaded GG@MPS@H, (d) MB-loaded GG@MPS@H, and (e) Cr^{6+}-loaded GG@MPS@H.

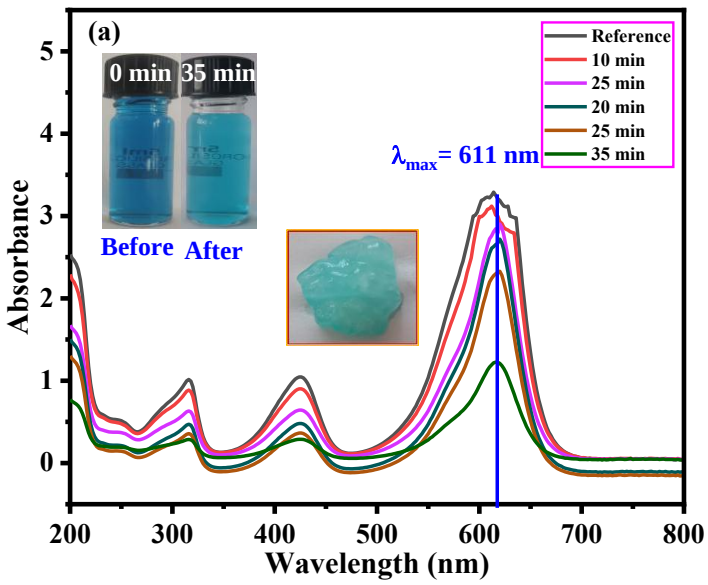
(a)
0 min
35 min
Before
After
λmax= 611 nm
Reference
10 min
25 min
20 min
25 min
35 min
Absorbance
Wavelength (nm)

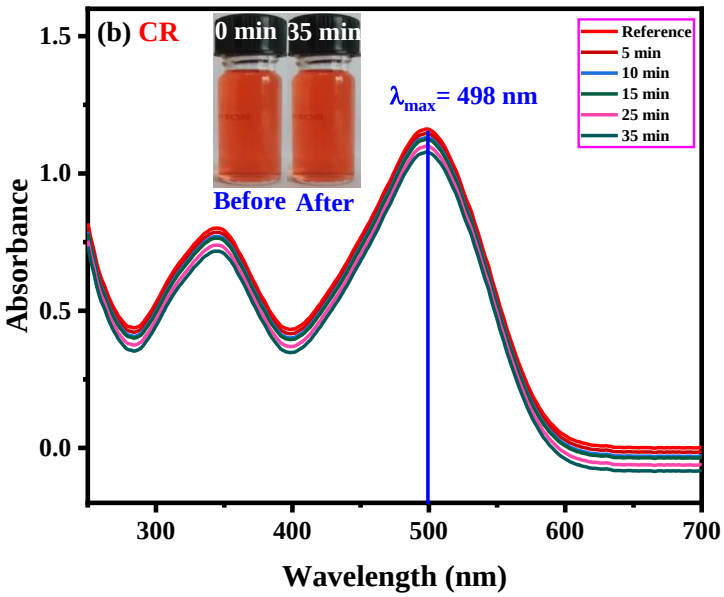
(b) CR
0 min
35 min
Before
After
λmax= 498 nm
Reference
5 min
10 min
15 min
25 min
35 min
Absorbance
Wavelength (nm)

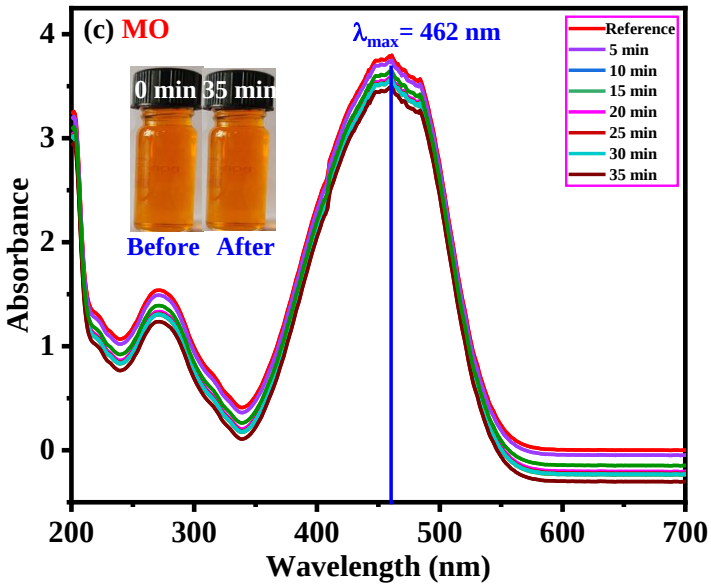
(c) MO
λmax= 462 nm
0 min
35 min
Before
After
Reference
5 min
10 min
15 min
20 min
25 min
30 min
35 min
Absorbance
Wavelength (nm)

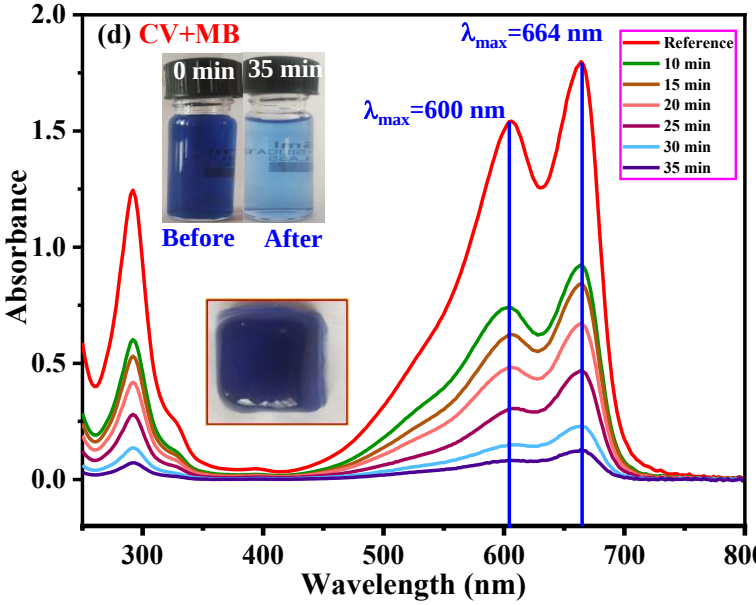
(d) CV+MB
λmax=664 nm
λmax=600 nm
0 min
35 min
Before
After
Reference
10 min
15 min
20 min
25 min
30 min
35 min
Absorbance
Wavelength (nm)

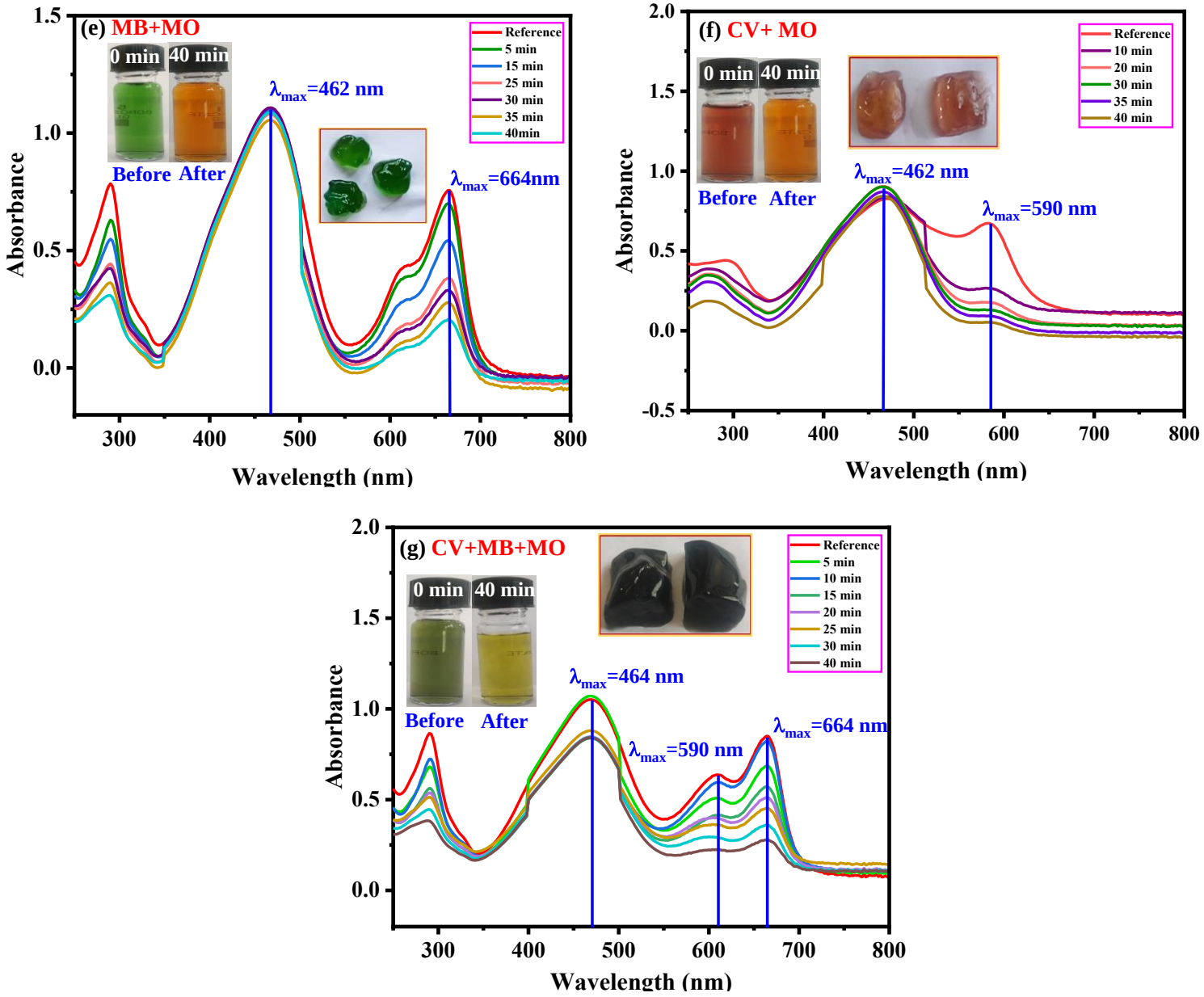

Fig. S3. The UV-vis spectrum and pictures of (a) individual MG dye removal, (b) individual anionic CR dye removal, (c) individual anionic MO dye remova, (d) binary of CV+MB, (e) binary mixture of MB+MO, (f) binary mixture of CV+MO, and ternary mixture (g) CV+MB+MO

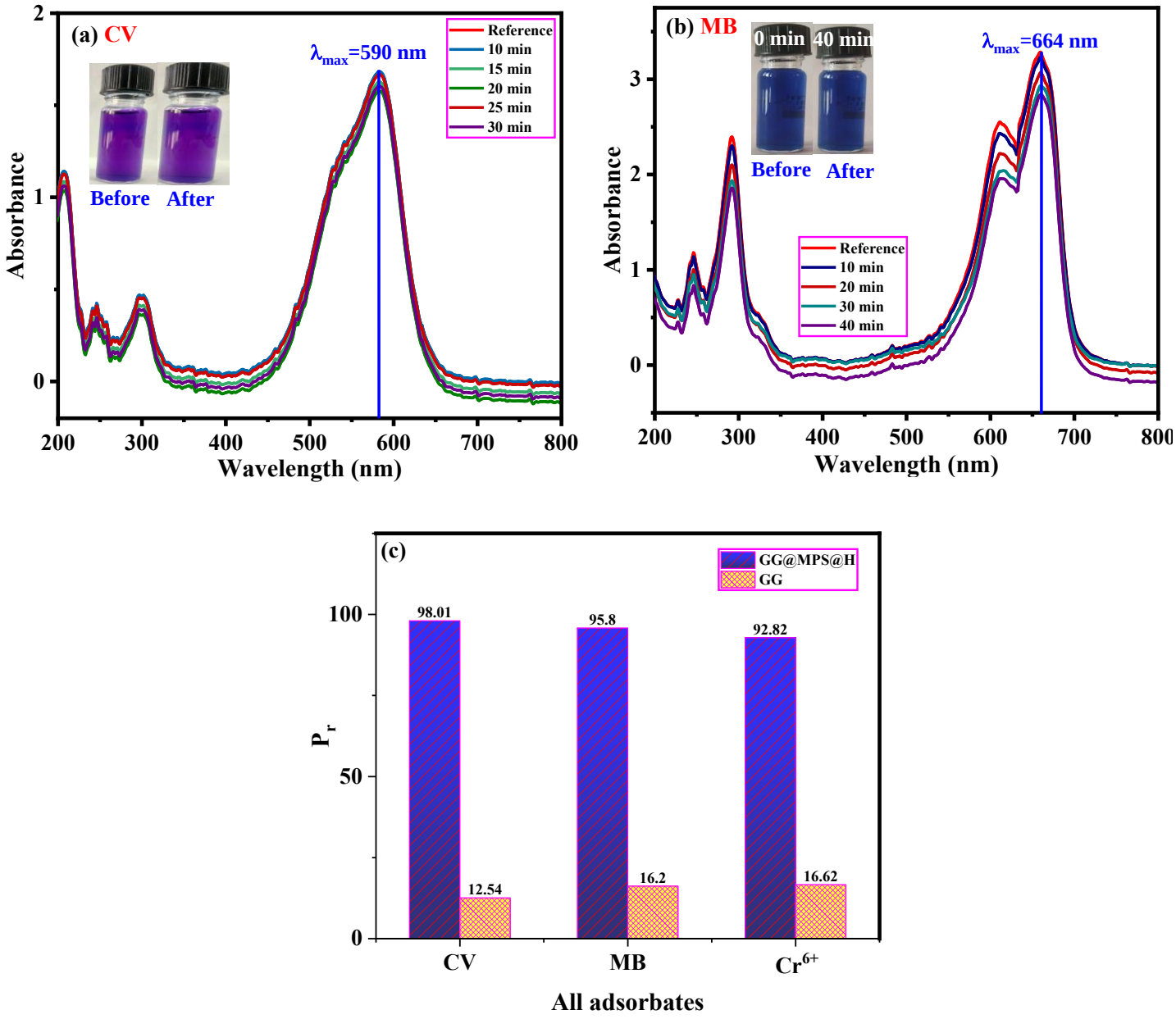

Fig. S4. (a) UV-vis spectrum of pristine GG for as adsorbent for CV removal, (b) UV-vis spectrum of pristine GG for MB removal, and (c) P_r of CV, MB, and Cr^{6+} ions by pristine GG

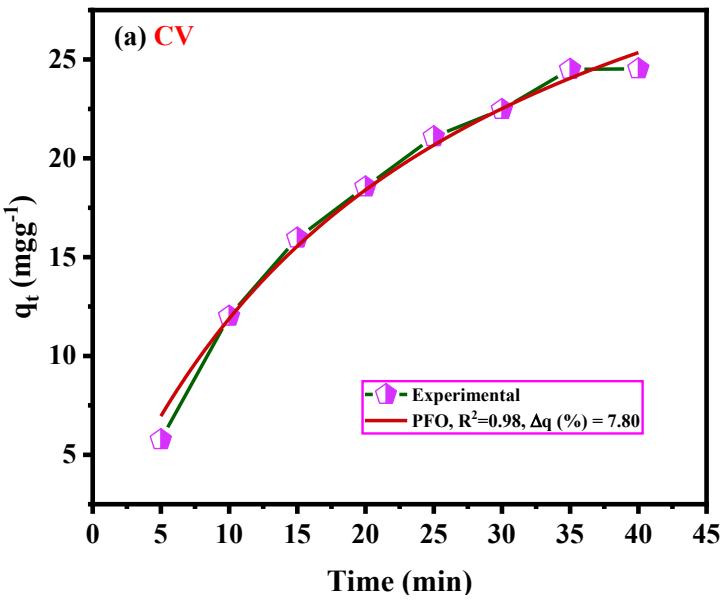
(a) CV
Experimental
PFO, R²=0.98, Δq (%) = 7.80
qt (mgg-1)
Time (min)

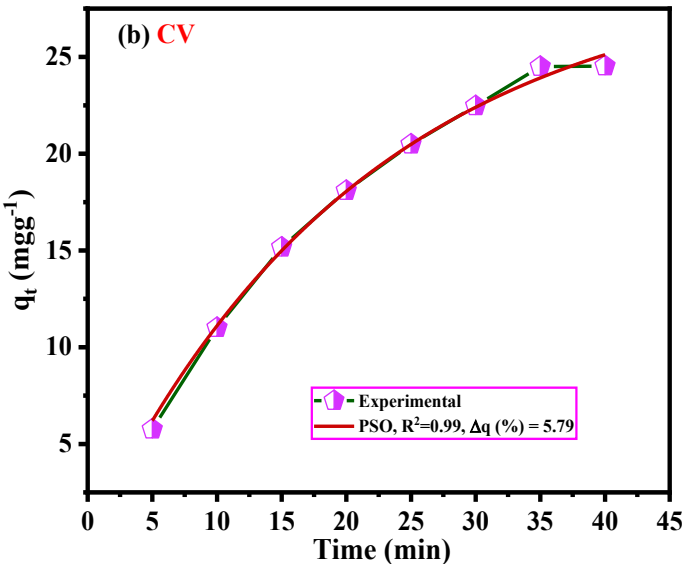
(b) CV
Experimental
PSO, R²=0.99, Δq (%) = 5.79
qt (mgg-1)
Time (min)

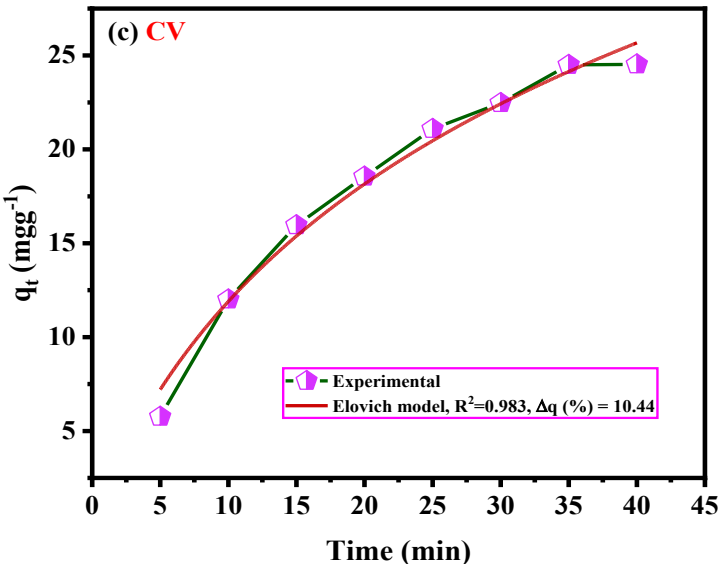
(c) CV
Experimental
Elovich model, R²=0.983, Δq (%) = 10.44
qt (mgg-1)
Time (min)

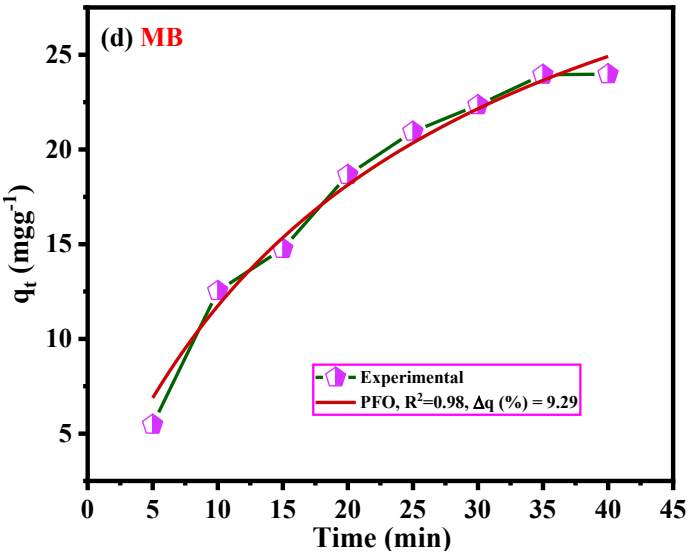
(d) MB
Experimental
PFO, R²=0.98, Δq (%) = 9.29
qt (mgg-1)
Time (min)

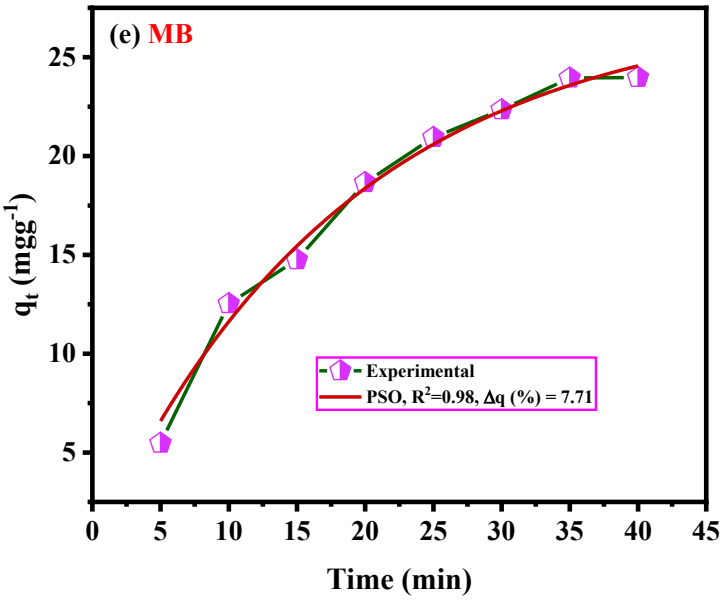
(e) MB
Experimental
PSO, R²=0.98, Δq (%) = 7.71
qt (mgg-1)
Time (min)

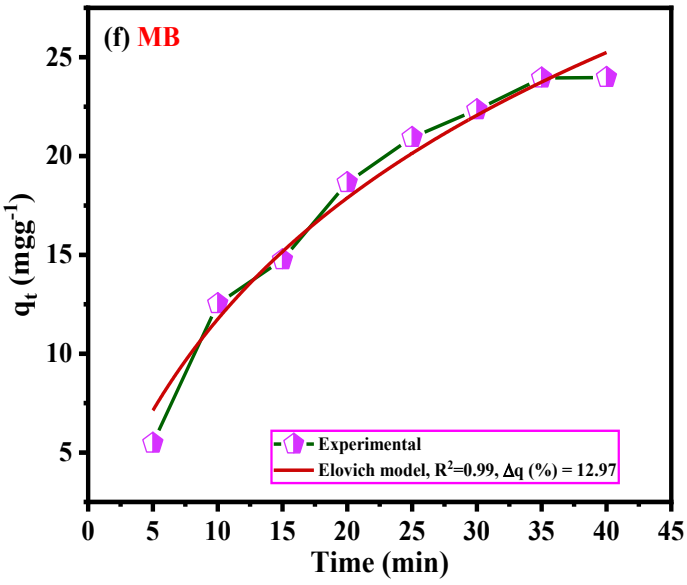
(f) MB
Experimental
Elovich model, R²=0.99, Δq (%) = 12.97
qt (mgg-1)
Time (min)

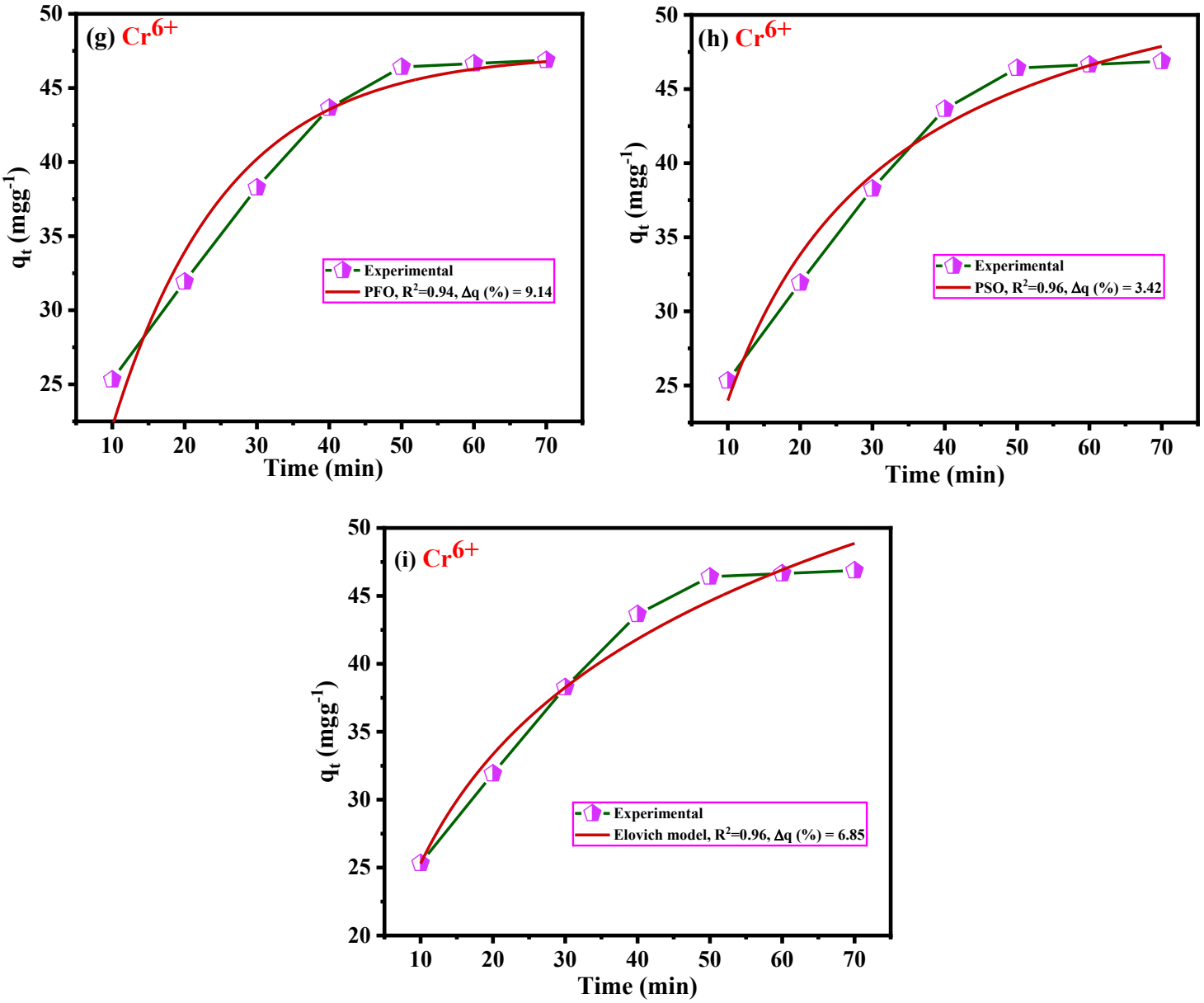

Fig. S5. Plots of different kinetic models of CV, MB and Cr^{6+} ions (a) PFO of CV, (b) PSO of CV, (c) Elovich of CV (d) PFO of MB, (e) PSO of MB, (f) Elovich of MB, (g) PFO of Cr^{6+} ions, (h) PSO of Cr^{6+} ions, and (i) Elovich of Cr^{6+} ions

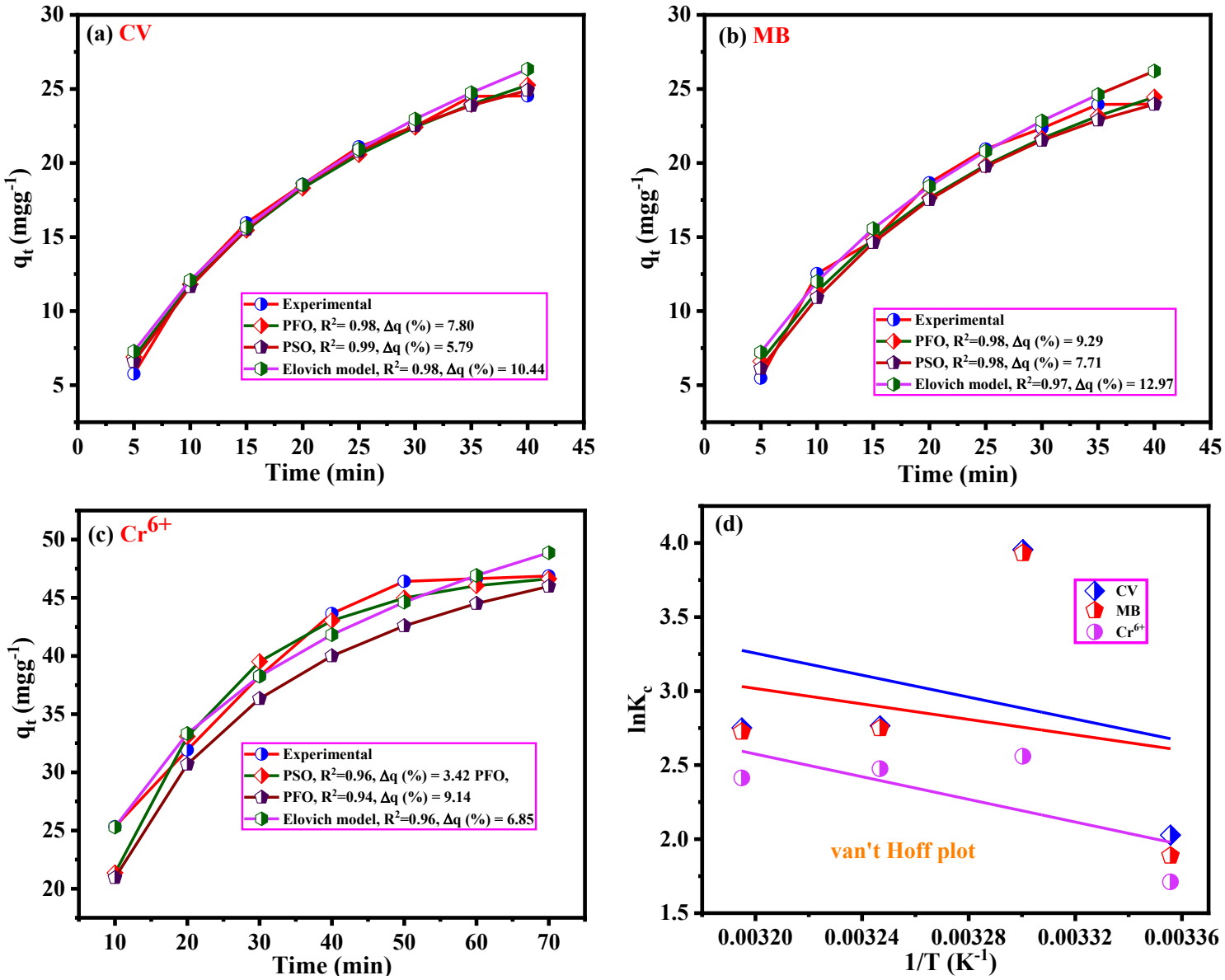

Fig. S6. Combined kinetic models and van't Hoff plot of CV, MB, and Cr^{6+} ions (a) kinetic model of CV (b) kinetic model of MB (c) kinetic model of Cr^{6+} ions (d) van't Hoff plot

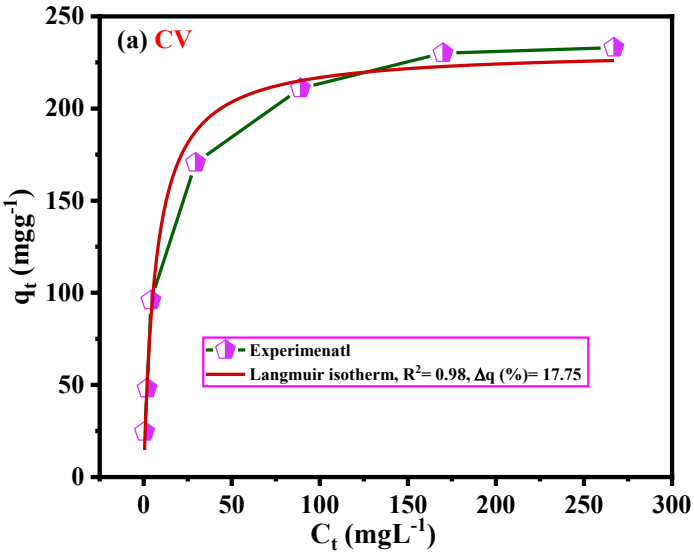
(a) CV
Experimenatl
Langmuir isotherm, R²= 0.98, Δq (%)= 17.75
qt (mgg-1)
Ct (mgL-1)

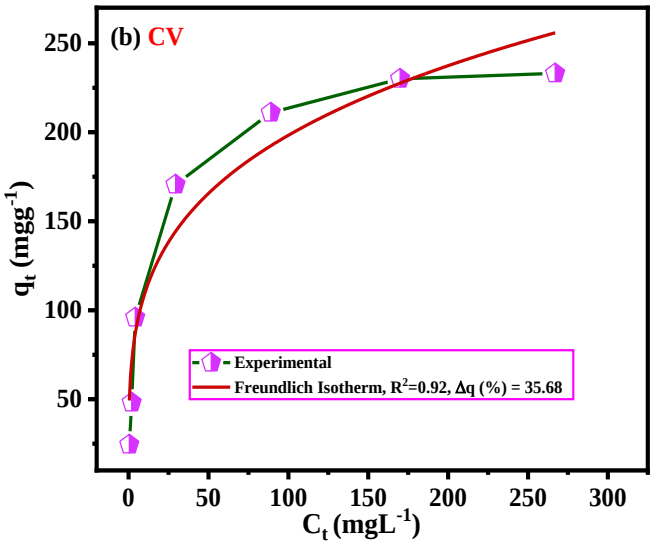
(b) CV
Experimental
Freundlich Isotherm, R²=0.92, Δq (%) = 35.68
qt (mgg-1)
Ct (mgL-1)

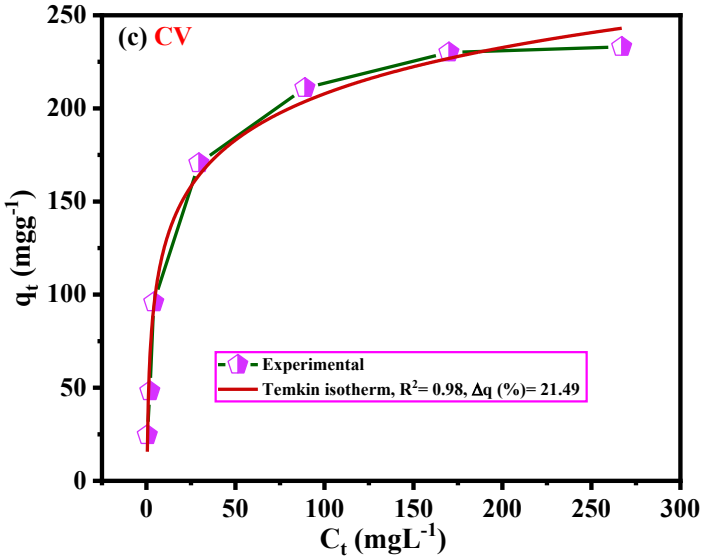
(c) CV
Experimental
Temkin isotherm, R²= 0.98, Δq (%)= 21.49
qt (mgg-1)
Ct (mgL-1)

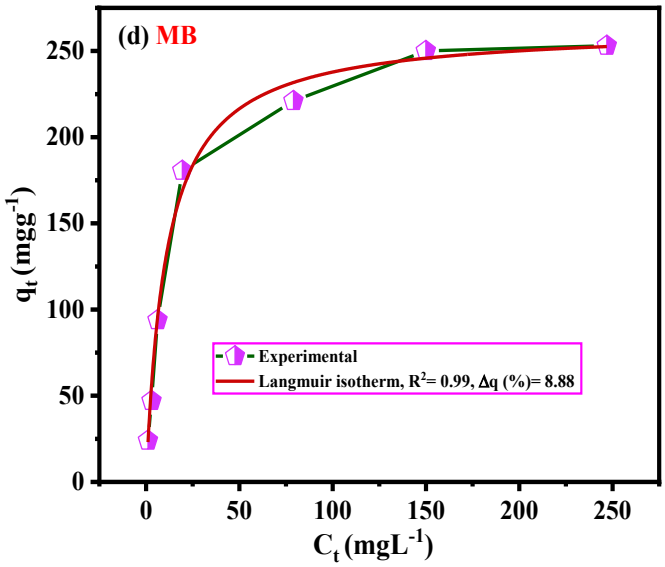
(d) MB
Experimental
Langmuir isotherm, R²= 0.99, Δq (%)= 8.88
qt (mgg-1)
Ct (mgL-1)

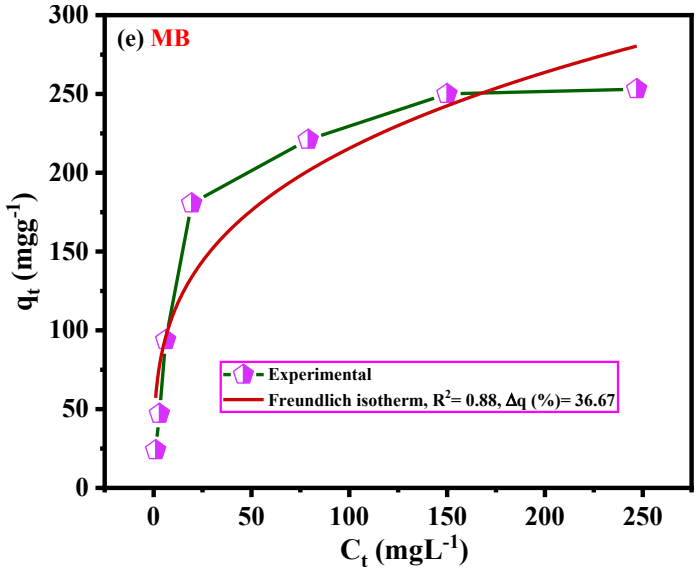
(e) MB
Experimental
Freundlich isotherm, R²= 0.88, Δq (%)= 36.67
qt (mgg-1)
Ct (mgL-1)

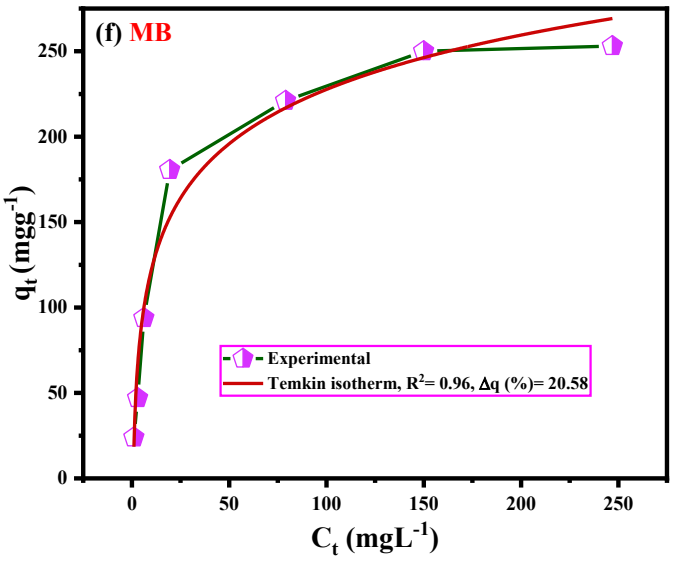
(f) MB
Experimental
Temkin isotherm, R²= 0.96, Δq (%)= 20.58
qt (mgg-1)
Ct (mgL-1)

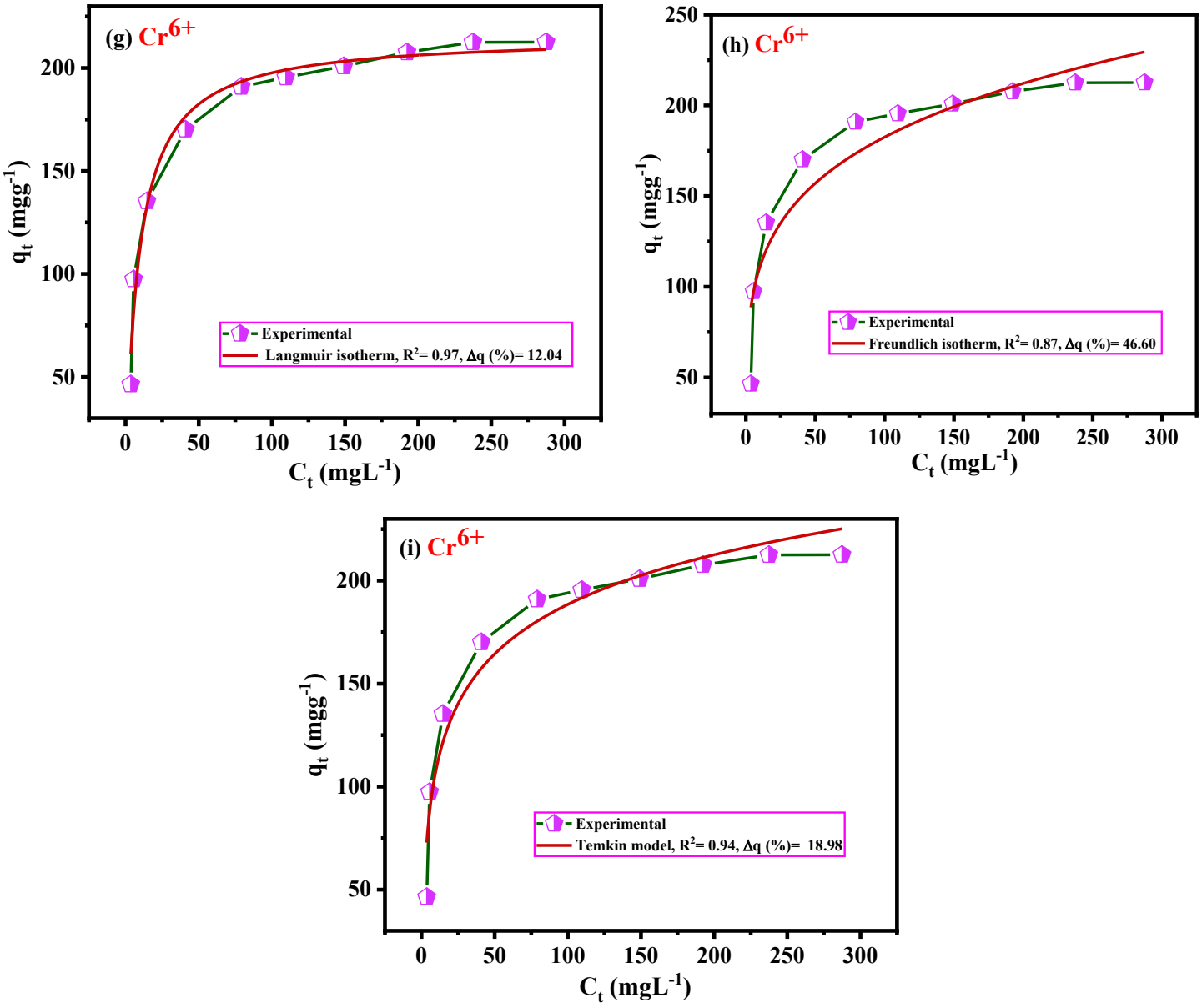

Fig. S7. Plots of different adsorption isotherm of CV, MB and Cr^{6+} ions (a) Langmuir isotherm of CV, (b) Freundlich isotherm of CV (c) Temkin isotherm of CV (d) Langmuir isotherm of MB (e) Freundlich isotherm of MB (f) Temkin isotherm of MB (g) Langmuir isotherm of Cr^{6+} ions (h) Freundlich isotherm of Cr^{6+} ions (i) Temkin isotherm of Cr^{6+} ions.

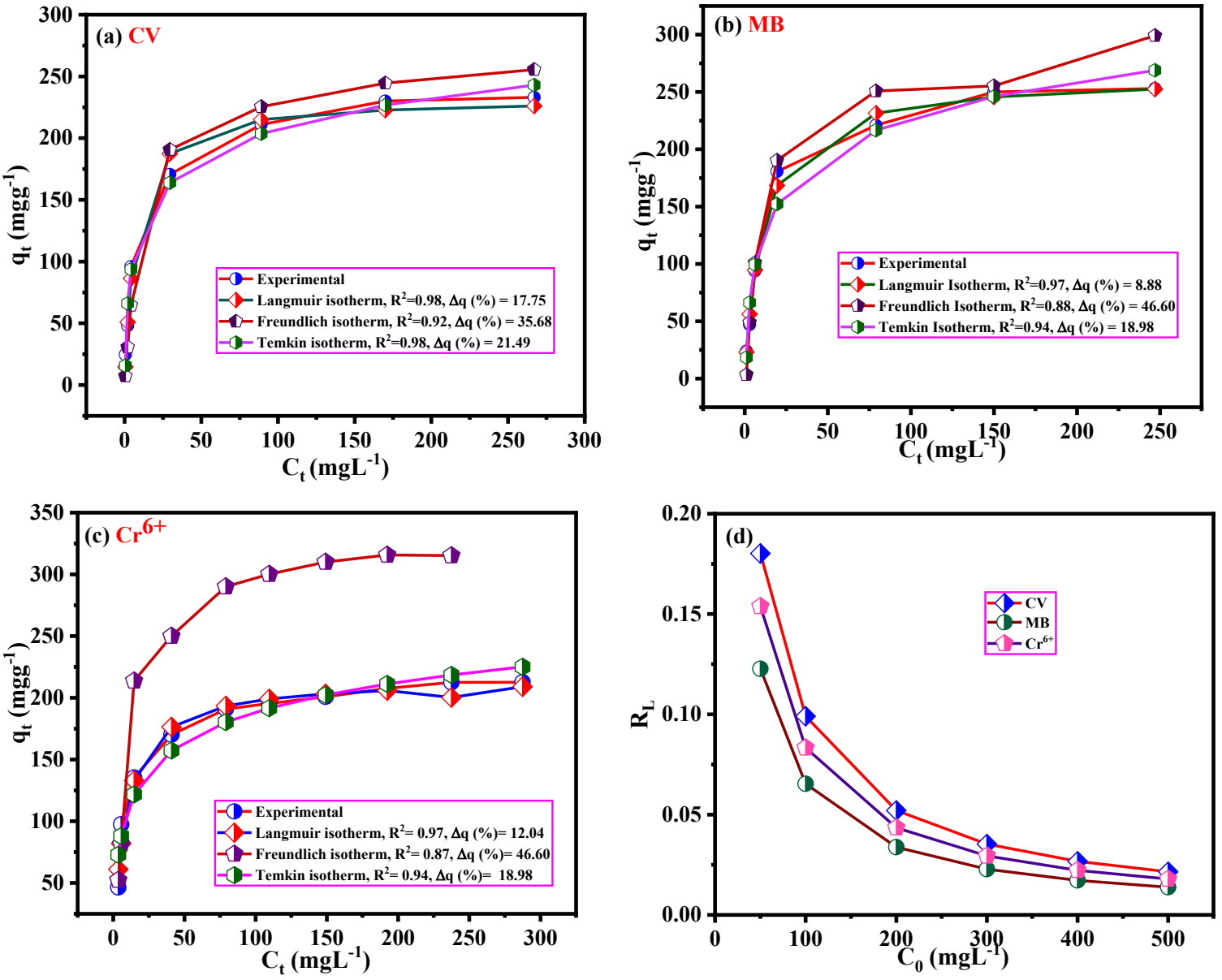

Fig. S8. Combined isotherm models of CV, MB, and Cr^{6+} ions (a) kinetic model of CV (b) kinetic model of MB (c) kinetic model of Cr^{6+} ions (d) C_0 vs R_L plot for all adsorbates.